Organic LETTERS

Letter

pubs.acs.org/OrgLett

Enantioselectivity in Catalytic Asymmetric Fischer Indolizations Hinges on the Competition of π-Stacking and CH/π Interactions

Trevor J. Seguin, Tongxiang Lu, and Steven E. Wheeler*

Department of Chemistry, Texas A&M University, College Station, Texas 77842, United States

Supporting Information

ABSTRACT: Computational analyses of the first catalytic asymmetric Fischer indolization (*J. Am. Chem. Soc.* **2011**, *133*, 18534) reveal that enantioselectivity arises from differences in hydrogen bonding and CH/π interactions between the substrate and catalyst in the operative transition states. This selectivity occurs despite strong π-stacking interactions that reduce the enantioselectivity.

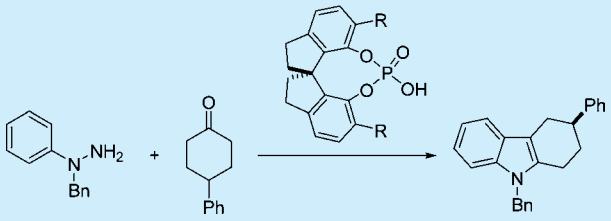

The use of phosphoric acids derived from chiral diols in organocatalysis has exploded since their introduction a decade ago.[1] However, for many such reactions, the mode of asymmetric induction is not fully understood, hindering the rational design of new catalysts. Herein, we use modern computational tools to unravel the impact of competing CH/π and π-stacking interactions on enantioselectivity in the first catalytic asymmetric Fischer indolization.[2]

The Fischer indole reaction[3] provides a popular route to indoline frameworks that occur widely in natural products.[4] However, until recently, there were no asymmetric versions of this reaction that were also catalytic. This changed in 2011, when List et al.[2] reported the first catalytic asymmetric indolization, using a chiral phosphoric acid catalyst derived from SPINOL (**1**, Scheme 1).[5] This provided a simple, mild, and efficient method for the enantioselective synthesis of highly diverse indoline scaffolds from simple starting materials. Their initial report utilized **1a** to catalyze the conversion of the *N*-protected hydrazone formed by the condensation of phenylhydrazines and 3-substituted cyclohexanones to the corresponding 3-substituted tetrahydrocarbazoles [eq 1].[2] Reported *er*'s generally exceeded 90:10 across a broad range of substrates. Other, similar catalysts, including **1b** and **1c**, as well as BINOL-derived catalysts such as **2b** and **2c**, provided significantly lower *er*'s for this reaction (see Table 1).

List et al.[6] later showed that SPINOL-derived phosphoric acids could also catalyze eq 2 to provide access to 3,3-disubstituted fused indolines. However, for these transformations, **1d** provided higher enantioselectivities than **1a**. Most recently, List and co-workers[7] showcased the utility of catalytic asymmetric indolizations in the first organocatalytic synthesis of helicenes [eq 3]. In this case, **1a** and **1d** proved suboptimal, and **1e** provided the highest *er*'s of the catalysts tested.[7]

That enantioselectivities in these Fischer indolizations[2,6,7] are highly sensitive to the identity of the pendant aryl groups suggests that subtle noncovalent interactions between the substrate and these aryl groups play a central role in enantioselectivity; identifying these noncovalent interactions is

Scheme 1

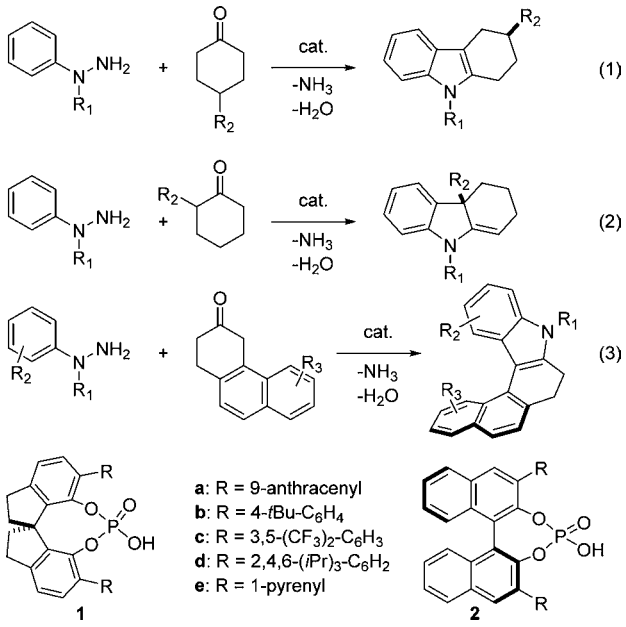

vital for the rational design of improved catalysts. Although pinpointing such interactions through experiment alone remains a challenge, computational quantum chemistry can provide key insights in such cases by identifying the noncovalent interactions at play in the stereocontrolling transition states (TSs).[8] Unfortunately, the impact of individual noncovalent interactions on the relative energies of competing transition states is rarely quantified.[8c,9]

The first reliable computational study of Brønsted acid promoted Fischer indolizations was not published until 2011, by Houk et al.[10] Others have used computations to study related

Received: May 7, 2015
Published: June 5, 2015

DOI: 10.1021/acs.orglett.5b01349
Org. Lett. 2015, 17, 3066−3069

Table 1. Experimental *er*'s (*S*:*R*), Corresponding Free Energy Barrier Differences (kcal mol^{-1}), and Predicted Relative Free Energy Barriers for Reaction 1 Catalyzed by 1a−c and 2b−c[a]

cat.	exptl *er*[b]	exptl $\Delta\Delta G^{\ddagger}$	theor $\Delta\Delta G^{\ddagger}$
1a	93.5:6.5	1.6	2.7
1b	43.5:56.5	−0.2	−0.1
1c	48.5:51.5	0.0	−0.9
2b	40.5:59.5	−0.2	−0.2
2c	59.5:40.5	0.2	0.1

[a] $\Delta\Delta G^{\ddagger} = \Delta G^{\ddagger}(R) - \Delta G^{\ddagger}(S)$ for the lowest-lying (*R*) and (*S*) transition states. [b] 5% catalyst at 30 °C in benzene.[2]

acid-catalyzed [3,3]-sigmatropic rearrangements in recent years,[11] building on the work of Goodman et al.[12] on chiral phosphoric acid catalyzed reactions. This includes recent work by Ess, Kürti et al.,[11a] and Tantillo and Tambar.[11b] Here, we use modern computational tools to quantify the impact of noncovalent interactions responsibe for the enantioselectivity of **1a** in the catalysis of eq 1 (R_1 = Bn, R_2 = Ph).

The stereocontrolling step in acid catalyzed Fischer indolizations is the [3,3]-sigmatropic rearrangement of the protonated ene-hydrazine arising from the tautomerization of the protonated hydrazone (Scheme 2).[6,11a,13] List et al.[2] proposed

Scheme 2

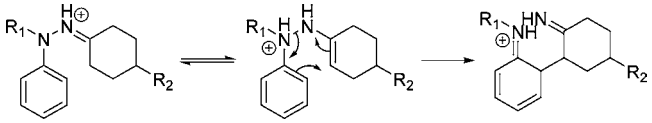

that the enantioselectivity for the catalysis of reaction 1 by **1a** arises from the more rapid [3,3]-sigmatropic rearrangement of one of the two diastereomeric ion pairs formed by the deprotonated catalyst and protonated ene-hydrazine. This is justified by the lack of C−C bond rotation in the resulting intermediate, as shown by Ess and Kürti.[11a]

To understand the origin of enantioselectivity in these reactions, computations were performed using Gaussian 09[14] at the ωB97X-D/6-311+G(d,p)//ωB97X-D/6-31G(d) level of theory.[15] This level of theory provides reliable predictions of reaction barriers for acid-catalyzed [3,3]-sigmatropic shifts, compared to recent benchmark values from Houk et al.,[10] while also capturing the subtle, dispersion-dominated noncovalent interactions that underlie the enantioselectivity of the studied catalytic reaction. Solvent effects (benzene) were accounted for in all computations (except where noted) using CPCM[16] with UAKS radii. Thermal free energy corrections were obtained at 303 K using standard rigid-rotor/harmonic oscillator approximations to compute partition functions. Structures were verified to be transition states based on the existence of a single imaginary vibration frequency.

In the presence of **1a**, we find that protonation of the ene-hydrazine preceding the [3,3]-sigmatropic rearrangement is exergonic by 6.7 kcal mol^{-1}. This proton transfer is crucial for reducing the activation energy of the rearrangement, consistent with previous work from Houk et al.[10] and Kürti et al.[11a] Following an extensive search of low-lying TS structures for this [3,3]-sigmatropic rearrangement catalyzed by **1a**, we identified the low-lying transition states responsible for formation of the (*S*) and (*R*) products (see Figure 1).

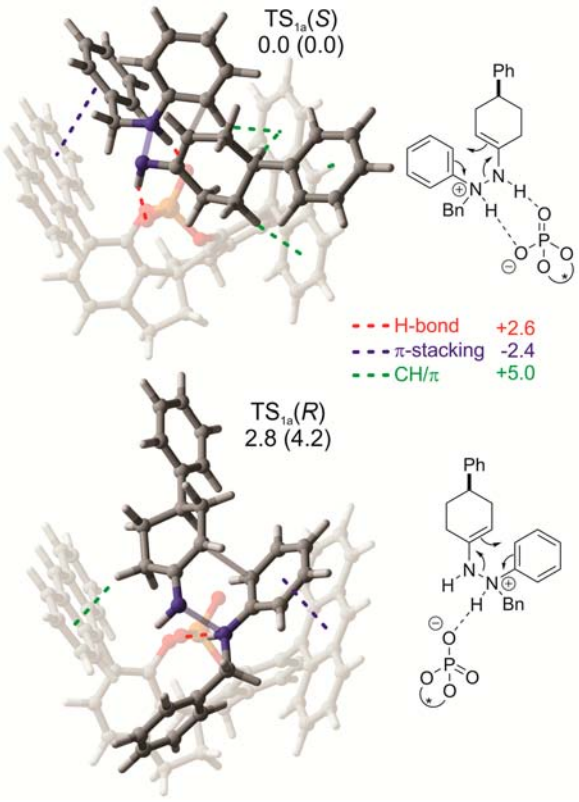

Figure 1. Lowest-lying [3,3]-sigmatropic rearrangement transition state structures leading to the (*S*) and (*R*) products for reaction 1 catalyzed by **1a**. Solution-phase relative free energies are provided, in kcal mol^{-1} (relative gas-phase energies, $\Delta\Delta E^{\ddagger}$, are given in parentheses). Key noncovalent interactions between substrate and catalyst are denoted with dashed lines. Approximate contributions of these interactions to $\Delta\Delta E^{\ddagger}$ are shown in kcal mol^{-1}.

In $TS_{1a}(S)$, the protonated substrate exhibits two NH-donated hydrogen bonds to the phosophoric acid, as expected.[2] On the other hand, $TS_{1a}(R)$ features only one NH-donated hydrogen bond. The other NH is directed toward one of the 9-anthracenyl substituents of the catalyst, although it is not in a position to engage in a favorable NH/π interaction.[17] The impact of these qualitative differences in hydrogen-bonding motifs on the enantioselectivity will be discussed below. Overall, we find that $TS_{1a}(R)$ is 2.7 kcal mol^{-1} higher in free energy than $TS_{1a}(S)$, which is a slight overestimation of the experimental enantioselectivity.[2] Computations provide even more reliable predictions for catalysis of reaction 1 by other chiral phosphoric acid catalysts (see Table 1). In particular, both the overall sense of stereoinduction and the magnitude of enantioselectivity are predicted very accurately for all but **1c**. In the case of **1c**, we predict modest enantioselectivity, whereas this catalyst was found to be unselective experimentally. Surprisingly, it is only for **2c** that the low-lying TS structures are structurally similar to those for **1a**.

Qualitatively, it is already apparent from Figure 1 that the structure of the substrate in $TS_{1a}(S)$ is more complementary to the chiral binding pocket of the catalyst, compared to that in $TS_{1a}(R)$. To understand the origin of the 2.7 kcal mol^{-1} difference in free energy between $TS_{1a}(R)$ and $TS_{1a}(S)$, we first note that the gas-phase energy difference, $\Delta\Delta E^{\ddagger}$, is 4.0 kcal mol^{-1}. In other words, entropic and solvent effects reduce the energy gap between these transition states by 1.3 kcal mol^{-1}. This

DOI: 10.1021/acs.orglett.5b01349
Org. Lett. 2015, 17, 3066−3069

4.0 kcal mol^{-1} difference in gas-phase energies between TS$_{1a}$(R) and TS$_{1a}$(S) can be decomposed into three components,[18]

$$\Delta\Delta E^{\ddagger} = \Delta\Delta E_{sub} + \Delta\Delta E_{cat} + \Delta\Delta E_{int}$$

where $\Delta\Delta E_{sub}$ is the difference in energy between the protonated ene-hydrazine substrate in the TS$_{1a}$(R) and TS$_{1a}$(S) geometries; $\Delta\Delta E_{cat}$ is the energy difference of the catalyst in these TS geometries; and $\Delta\Delta E_{int}$ is the difference in interaction energies between the catalyst and substrate in these TS geometries. These components of $\Delta\Delta E^{\ddagger}$ are depicted in Figure 2a.

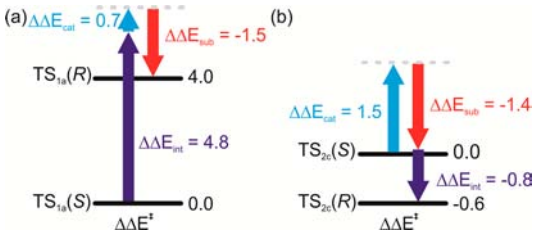

Figure 2. (a) Decomposition of the energy difference between TS$_{1a}$(R) and TS$_{1a}$(S), $\Delta\Delta E^{\ddagger}$, into contributions from the difference in energy of the substrate ($\Delta\Delta E_{sub}$), the difference in energy of the catalyst ($\Delta\Delta E_{cat}$), and the difference in interaction energies of the substrate with the catalyst ($\Delta\Delta E_{int}$), in kcal mol^{-1}; (b) analogous decomposition of the energy difference between TS$_{2c}$(R) and TS$_{2c}$(S).

First, we note that $\Delta\Delta E_{sub}$ is negative—the substrate in TS$_{1a}$(R) is 1.5 kcal mol^{-1} lower in energy than that in TS$_{1a}$(S). This presumably arises from the more favorable *anti* conformation of the benzyl substituent in TS$_{1a}$(R), compared to the *gauche* conformer in TS$_{1a}$(S) (see SI for more details). These effects are overshadowed by the +4.8 kcal mol^{-1} difference in $\Delta\Delta E_{int}$, which, when combined with the +0.7 kcal mol^{-1} contribution from $\Delta\Delta E_{cat}$, leads to the 4.0 kcal mol^{-1} total difference in energy between TS$_{1a}$(R) and TS$_{1a}$(S). Thus, the enantioselectivity of **1a** arises from the more favorable binding of the (S)-substrate than the (R)-substrate by **1a** in the TS for the [3,3] sigmatropic rearrangement, as proposed by List et al.[2] However, this effect is tempered by the energetic cost of adopting the less favorable *syn* conformation of the substrate in TS$_{1a}$(S).

There are myriad noncovalent interactions present in TS$_{1a}$(S) and TS$_{1a}$(R) whose net effect leads to the 4.8 kcal mol^{-1} difference in interaction energies (see Figure 1); unraveling the contributions of these interactions is impossible by simply examining the structures. To understand this difference, we approximately decomposed $\Delta\Delta E_{int}$ into contributions from noncovalent interactions between the substrate and the three components of the catalyst (see Figure 1). Briefly, we partitioned the catalyst into three pieces by severing the C−C bonds connecting the two anthracenyl groups with the phosphoric acid "core", capping the open valences with hydrogen atoms.[9a] We then evaluated the interaction of the (S) and (R) transition state structures with each of these three catalyst components, providing an estimate of the H-bond interaction with the phosphoric acid functionality and the π-stacking and CH/π interactions with the two anthracenyl groups.

First, the qualitatively different hydrogen bonding interactions present in TS$_{1a}$(R) and TS$_{1a}$(S) contribute 2.6 kcal mol^{-1} to $\Delta\Delta E_{int}$, preferentially stabilizing TS$_{1a}$(S) over TS$_{1a}$(R). However, the enantioselectivity of **1a** does not arise from this difference alone; there are also substantial contributions from noncovalent interactions of the substrate with the anthracenyl groups. The most prominent interactions with the anthracenyl groups in these structures are π-stacking interactions.[19] For TS$_{1a}$(S), these stacking interactions involve the benzyl *N*-protecting group, while in TS$_{1a}$(R) the stacking interaction involves the phenyl ring of the phenyl hydrazine. These interactions contribute −2.4 kcal mol^{-1} to $\Delta\Delta E_{int}$. That is, π-stacking interactions of the substrate with the 9-anthracenyl group preferentially stabilize TS$_{1a}$(R), significantly reducing the energy gap between TS$_{1a}$(R) and TS$_{1a}$(S)!

The effects of π-stacking interactions are overcome by the difference in favorable CH/π interactions between the substrate and the other 9-anthracenyl group, which contributes 5.0 kcal mol^{-1} to $\Delta\Delta E_{int}$. In particular, in TS$_{1a}$(S) there are aliphatic CH/π interactions of the cyclohexenyl ring with the 9-anthracenyl groups as well as aromatic CH/π interactions (edge-to-face interactions)[20] of the phenyl ring of the phenyl hydrazine with the anthracenyl group. These interactions outweigh the single CH/π contact in TS$_{1a}$(R); in TS$_{1a}$(R), the substrate simply does not fit sufficiently tightly in the bonding pocket of **1a** to engage in favorable CH/π interactions with one anthracenyl group while maintaining π-stacking interactions with the other. This occurs in part because of the *anti* conformation of the substrate in TS$_{1a}$(R). These energy differences are consistent with analyses based on the NCI index of Yang and co-workers,[21] which indicate more extensive dispersion-like interactions between the substrate and the 9-anthracenyl group in TS$_{1a}$(S), compared to TS$_{1a}$(R) (see SI Figure S1).

This can be contrasted with the TS structures for **2c**, for which the lowest-lying (S) transition state [TS$_{2c}$(S)] exhibits the same *gauche* conformation as TS$_{1a}$(S), and the lowest-lying (R) transition state [TS$_{2c}$(R)] exhibits only a single NH-donated hydrogen bond. First, in the gas phase TS$_{2c}$(R) is 0.6 kcal mol^{-1} lower in energy than TS$_{2c}$(S). This −0.6 kcal mol^{-1} energy difference is decomposed in Figure 2b. In this case, $\Delta\Delta E_{int}$ is −0.8 kcal mol^{-1}; the H-bonding, π-stacking, and CH/π interactions between the substrate and catalyst are mostly balanced, slightly favoring the transition state leading to the (R) product. This difference is compensated by entropic and solvent effects, leading to the 0.1 kcal mol^{-1} difference in free energy between TS$_{2c}$(R) and TS$_{2c}$(S).

In conclusion, we have shown that the marked enantioselectivity exhibited by the first catalytic asymmetric Fischer indolization[2] arises from differences in hydrogen bonding as well as favorable CH/π interactions in the rate-limiting [3,3]-sigmatropic rearrangement. The latter effect derives from the shape complementarity of the substrate and the binding pocket of **1a** and echoes recent work from Jindal and Sunoj[8h] on a chiral phosphoric acid catalyzed asymmetric sulfoxidation reaction[22] as well as the phosphoric acid catalyzed indole aza-Claisen reaction reported by Tantillo and Tambar.[11b] Vital to this shape complementarity is the *gauche* conformation of the benzyl group in the (S) transition state. The energetic cost of adopting this less-favorable conformation is more than compensated by the stronger noncovalent interactions that result. Furthermore, even though strong π-stacking interactions occur in both TS structures, their effect is to reduce the enantioselectivity of this reaction by preferentially stabilizing TS$_{1a}$(R). These data underscore the challenge of rationally designing catalysts that engage in the many coordinated noncovalent interactions required to achieve significant stabilization of a particular transition state,[8b] as well as the power of CH/π interactions as a means of achieving asymmetric induction.[8h,11b] Whether similar effects are responsible for the enantioselectivity of

DOI: 10.1021/acs.orglett.5b01349
Org. Lett. 2015, 17, 3066−3069

reactions 2 and 3 remains to be seen. Regardless, these results constitute a key first step toward a general understanding of asymmetric induction in chiral phosphoric acid catalyzed Fischer indolizations,[2,6,7] which should aid the further development of organocatalysts for this transformation.

■ ASSOCIATED CONTENT

Supporting Information

Additional computational details, computed energies and free energies, Cartesian coordinates. The Supporting Information is available free of charge on the ACS Publications website at DOI: 10.1021/acs.orglett.5b01349.

■ AUTHOR INFORMATION

Corresponding Author

*E-mail: wheeler@chem.tamu.edu.

Notes

The authors declare no competing financial interest.

■ ACKNOWLEDGMENTS

This work was supported by The Welch Foundation (Grant A-1775) and the National Science Foundation (Grant CHE-1266022). We also acknowledge the Texas A&M Supercomputing Facility for computational resources. Molecular structure figures were generated using CYLview.[23]

■ REFERENCES

(1) (a) Akiyama, T. *Chem. Rev.* **2007**, *107*, 5744−5758. (b) Kampen, D.; Reisinger, C. M.; List, B. *Top. Curr. Chem.* **2010**, *291*, 395−456. (c) Tereda, M. *Synthesis* **2010**, 1929−1982. (d) Parmar, D.; Sugiono, E.; Raja, S.; Rueping, M. *Chem. Rev.* **2014**, *114*, 9047−9153.

(2) Müller, S.; Webber, M. J.; List, B. *J. Am. Chem. Soc.* **2011**, *133*, 18534−18437.

(3) (a) Fischer, E.; Jourdan, F. *Ber. Dtsch. Chem. Ges.* **1883**, *16*, 2241−2245. (b) Fischer, E.; Hess, O. *O. Ber. Dtsch. Chem. Ges.* **1884**, *17*, 559−568.

(4) (a) Gribble, G. W. *J. Chem. Soc., Perkin Trans. 1* **2000**, 1045−1075. (b) Humprey, G. R.; Kuethe, J. T. *Chem. Rev.* **2006**, *106*, 2875−2911.

(5) (a) Xu, F.; Huang, D.; Han, C.; Shen, W.; Lin, X.; Wang, Y. *J. Org. Chem.* **2010**, *75*, 8677−8680. (b) Čorić, I.; Müller, S.; List, B. *J. Am. Chem. Soc.* **2010**, *132*, 17370−17373. (c) Xing, C.-H.; Liao, Y.-X.; Ng, J.; Hu, Q.-S. *J. Org. Chem.* **2011**, *76*, 4125−4131.

(6) Martínez, A.; Webber, M. J.; Müller, S.; List, B. *Angew. Chem., Int. Ed.* **2013**, *52*, 9486−9490.

(7) Kötzner, L.; Martínez, A.; De Fusco, C.; List, B. *Angew. Chem., Int. Ed.* **2014**, *53*, 5202−5205.

(8) (a) Houk, K. N.; Cheong, P. H.-Y. *Nature* **2008**, *455*, 309−313. (b) Knowles, R. R.; Jacobsen, E. N. *Proc. Natl. Acad. Sci. U.S.A.* **2010**, *107*, 20678−20685. (c) Krenske, E. H.; Houk, K. N. *Acc. Chem. Res.* **2013**, *46*, 979−989. (d) Uyeda, C.; Jacobsen, E. N. *J. Am. Chem. Soc.* **2011**, *133*, 5062−5075. (e) Holland, M. C.; Paul, S.; Schweizer, W. B.; Bergander, K.; Mück-Lichtenfeld, C.; Lakhdar, S.; Mayr, H.; Gilmour, R. *Angew. Chem., Int. Ed.* **2013**, *52*, 7967−7971. (f) Johnston, R. C.; Cheong, P. H.-Y. *Org. Biomol. Chem.* **2013**, *11*, 5057−5064. (g) Allen, S. E.; Mahatthananchai, J.; Bode, J. W.; Kozlowski, M. C. *J. Am. Chem. Soc.* **2012**, *134*, 12098−12103. (h) Jindal, G.; Sunoj, R. B. *Angew. Chem., Int. Ed.* **2014**, *53*, 4432−4436. (i) Odagi, M.; Furukori, K.; Yamamoto, Y.; Sato, M.; Iida, K.; Yamanaka, M.; Nagasawa, K. *J. Am. Chem. Soc.* **2015**, *137*, 1909−1915.

(9) (a) Lu, T.; Zhu, R.; An, Y.; Wheeler, S. E. *J. Am. Chem. Soc.* **2012**, *134*, 3095−3102. (b) Johnston, C. P.; Kothari, A.; Sergeieva, T.; Okovytyy, S. I.; Jackson, K. E.; Paton, R. S.; Smith, M. D. *Nat. Chem.* **2015**, *7*, 171−177. (c) Carrillo, R.; López-Rodríguez, M.; Martín, V. S.; Martín, T. *Angew. Chem., Int. Ed.* **2009**, *48*, 7803−7808.

(10) Çelebi-Ölçüm, N.; Boal, B. W.; Huters, A. D.; Garg, N. K.; Houk, K. N. *J. Am. Chem. Soc.* **2011**, *133*, 5752−5755.

(11) (a) Li, G.-Q.; Gao, H.; Keene, C.; Devonas, M.; Ess, D. H.; Kürti, L. *J. Am. Chem. Soc.* **2013**, *135*, 7414−7417. (b) Maity, P.; Pemberton, R. P.; Tantillo, D. J.; Tambar, U. K. *J. Am. Chem. Soc.* **2013**, *135*, 16380−16383.

(12) (a) Simón, L.; Goodman, J. M. *J. Am. Chem. Soc.* **2008**, *130*, 8741−8747. (b) Simón, L.; Goodman, J. M. *J. Am. Chem. Soc.* **2009**, *131*, 4070−4077. (c) Simón, L.; Goodman, J. M. *J. Org. Chem.* **2010**, *75*, 589−597. (d) Simón, L.; Goodman, J. M. *J. Org. Chem.* **2011**, *76*, 1775−1788. (e) Grayson, M. N.; Pellegrinet, S. C.; Goodman, J. M. *J. Am. Chem. Soc.* **2012**, *134*, 2716−2722. (f) Overvoorde, L. M.; Grayson, M. N.; Luo, Y.; Goodman, J. M. *J. Org. Chem.* **2015**, *80*, 2634−2640.

(13) Robinson, G. M.; Robinson, R. *J. Chem. Soc. Trans* **1924**, *125*, 827−840.

(14) Frisch, M. J.; Trucks, G. W.; Schlegel, H. B.; Scuseria, G. E.; Robb, M. A.; Cheeseman, J. R.; Scalmani, G.; Barone, V.; Mennucci, B.; Petersson, G. A.; Nakatsuji, H.; Caricato, M.; Li, X.; Hratchian, H. P.; Izmaylov, A. F.; Bloino, J.; Zheng, G.; Sonnenberg, J. L.; Hada, M.; Ehara, M.; Toyota, K.; Fukuda, R.; Hasegawa, J.; Ishida, M.; Nakajima, T.; Honda, Y.; Kitao, O.; Nakai, H.; Vreven, T.; Montgomery, J. A., Jr.; Peralta, J. E.; Ogliaro, F.; Bearpark, M.; Heyd, J. J.; Brothers, E.; Kudin, K. N.; Staroverov, V. N.; Kobayashi, R.; Normand, J.; Raghavachari, K.; Rendell, A.; Burant, J. C.; Iyengar, S. S.; Tomasi, J.; Cossi, M.; Rega, N.; Millam, N. J.; Klene, M.; Knox, J. E.; Cross, J. B.; Bakken, V.; Adamo, C.; Jaramillo, J.; Gomperts, R.; Stratmann, R. E.; Yazyev, O.; Austin, A. J.; Cammi, R.; Pomelli, C.; Ochterski, J. W.; Martin, R. L.; Morokuma, K.; Zakrzewski, V. G.; Voth, G. A.; Salvador, P.; Dannenberg, J. J.; Dapprich, S.; Daniels, A. D.; Farkas, Ö.; Foresman, J. B.; Ortiz, J. V.; Cioslowski, J.; Fox, D. J. *Gaussian 09*, revision D.01; Gaussian, Inc.: Wallingford, CT, 2009.

(15) Chai, J.-D.; Head-Gordon, M. *J. Chem. Phys.* **2008**, *128*, 084106.

(16) (a) Barone, V.; Cossi, M. *J. Phys. Chem. A* **1998**, *102*, 1995−2001. (b) Cossi, M.; Rega, N.; Scalmani, G.; Barone, V. *J. Comput. Chem.* **2003**, *24*, 669−681.

(17) The free energy of the lowest-lying (*R*)-transition state featuring dual NH-donated hydrogen bonds to the phosphoric acid is 7.3 kcal mol^{-1}, relative to $TS_{1a}(S)$.

(18) This decomposition is similar in spirit, but different in aim, than the distortion−interaction analyses utilized by Houk and co-workers and the activation-strain model of Bickelhaupt et al.; see: (a) Ess, D. H.; Houk, K. N. *J. Am. Chem. Soc.* **2007**, *129*, 10646. (b) van Zeist, W.-J.; Bickelhaupt, F. M. *Org. Biomol. Chem.* **2010**, *8*, 3118.

(19) (a) Wheeler, S. E. *Acc. Chem. Res.* **2013**, *46*, 1029−1038. (b) Wheeler, S. E.; Bloom, J. W. G. *J. Phys. Chem. A* **2014**, *118*, 6133−6147.

(20) (a) Meyer, E. A.; Castellano, R. K.; Diederich, F. *Angew. Chem., Int. Ed.* **2003**, *42*, 1210−1250. (b) Salonen, L. M.; Ellermann, M.; Diederich, F. *Angew. Chem., Int. Ed.* **2011**, *50*, 4808−4842. (c) Raju, R. K.; Bloom, J. W. G.; An, Y.; Wheeler, S. E. *ChemPhysChem* **2011**, *12*, 3116−3130. (d) Bloom, J. W. G.; Raju, R. K.; Wheeler, S. E. *J. Chem. Theory and Comput.* **2012**, *8*, 3167−3174. (e) Wheeler, S. E.; Houk, K. N. *Mol. Phys.* **2009**, *107*, 749−760. (f) Plevin, M. J.; Bryce, D. L.; Boisbouvier, J. *Nat. Chem.* **2010**, *2*, 466−471.

(21) Johnson, E. R.; Keinan, S.; Mori-Sánchez, P.; Contreras-García; Cohen, A. J.; Yang, W. *J. Am. Chem. Soc.* **2010**, *132*, 6498−6506.

(22) Liao, S.; Čorić, I.; Wang, Q.; List, B. *J. Am. Chem. Soc.* **2012**, *134*, 10765−10768.

(23) *CYLview*, 1.0b; Legault, C. Y., Université de Sherbrooke, 2009 (http://www.cylview.org).

DOI: 10.1021/acs.orglett.5b01349
Org. Lett. 2015, 17, 3066−3069